

Wetting and superhydrophobic properties of PECVD grown hydrocarbon and fluorinated-hydrocarbon coatings

D.K. Sarkar^a, M. Farzaneh^a, R.W. Paynter^b

^a Canada Research Chair on Atmospheric Icing Engineering of Power Networks (INGIVRE) and Industrial Chair on Atmospheric Icing of Power Network Equipment (CIGELE), Université du Québec à Chicoutimi (UQAC), 555 Boulevard de l'Université, Chicoutimi, Québec, G7H 2B1, Canada

^b INRS-ÉMT, 1650 boul. Lionel-Boulet, Varennes, Québec, J3X 1S2, Canada

Received 7 August 2009, Accepted 16 December 2009, Available online 4 January 2010
doi:10.1016/j.apsusc.2009.12.049

Abstract

Wetting characteristics of micro-nanorough substrates of aluminum and smooth silicon substrates have been studied and compared by depositing hydrocarbon and fluorinated-hydrocarbon coatings via plasma enhanced chemical vapor deposition (PECVD) technique using a mixture of Ar, CH₄ and C₂F₆ gases. The water contact angles on the hydrocarbon and fluorinated-hydrocarbon coatings deposited on silicon substrates were found to be 72° and 105°, respectively. However, the micro-nanorough aluminum substrates demonstrated superhydrophobic properties upon coatings with fluorinated-hydrocarbon providing a water contact angle of ~165° and contact angle hysteresis below 2° with water drops rolling off from those surfaces while the same substrates showed contact angle of 135° with water drops sticking on those surfaces. The superhydrophobic properties is due to the high fluorine content in the fluorinated-hydrocarbon coatings of ~36 at.%, as investigated by X-ray photoelectron spectroscopy (XPS), by lowering the surface energy of the micro-nanorough aluminum substrates.

PACS

68.37.-d, 68.37.Ps, 68.08.Bc

Keywords : Superhydrophobic; Fluorinated-hydrocarbon coatings; AFM; SEM

1. Introduction

Superhydrophobicity, a property steering the development of nature inspired technology and solutions, has lately become a very popular field for its wide range of uses in diverse areas. The most common areas where superhydrophobic surfaces attract attention include anti-biofouling paints for boats [1], bio-chips [2], biomedical applications [3], microfluidics [4], corrosion resistance [5], eyeglasses, self-cleaning windshields for automobiles [6], stain resistant textiles [7], anti-sticking of snow for antennas and windows [8], expected inhibition of adherence of snow, oxidation, current conduction [9] and many others.

A surface, such as that of lotus leaves [10], exhibiting nearly zero wetting is termed "superhydrophobic". The zero wetting on lotus leaves surface is mainly due to the presence of a micro-nanorough pattern on their surface which is again covered with a low surface energy waxy coating. The micro-nanorough pattern allows large amount of air entrapment making it a heterogeneous surface composite of air and the surface where the air and the waxy tissue contributes to low surface energy weakening its interaction with water and therefore enhancing the water contact angle with its surface. The behavior of rolling water drops on lotus leaves' surface can be compared with the Cassie–Baxter model which explains the effect of roughness as well as air entrapment on enhancing water contact angle values making the area fraction of the solid in contact with the drop negligible [11].

Nature's such profitable wonder has inspired researchers around the world to replicate its water repellency for the various aforementioned but not limited uses using variety of techniques [6] and [12]. In recent years, our group has been extensively working on the superhydrophobic coatings for its applications in the areas where reduction of ice adhesion is of importance [13], [14], [15], [16], [17], [18] and [19]. The above works are fundamentally based on two step process where initially a rough pattern was created and the rough surface either passivated with fluoroalkylsilane [17] or stearic acid molecules [13], [17], [18] and [19] or coated with rf-sputtered Teflon [15]. Very recently, we have demonstrated that rf-sputtered Teflon coated etched aluminum surfaces are highly superhydrophobic [15]. We have also produced fluorinated-hydrocarbon coatings and demonstrated the formation of fluorinated-hydrocarbon nano-rings using nanosphere lithography (NSL) [16]. In the present work, we have deposited fluorinated-hydrocarbon coatings on different substrates and have studied their wetting and

superhydrophobic properties. We have also compared the wetting characteristics with those substrates coated with hydrocarbon coatings.

2. Experiment

Hydrocarbon and fluorinated-hydrocarbon coatings were performed using an inductively coupled plasma enhanced chemical vapor deposition (PECVD) applying a power of 100 W in the RF source using a mixture of Ar and CH₄ for hydrocarbon and Ar, CH₄ and C₂F₆ for fluorinated-hydrocarbon coatings [16]. The high vacuum chamber was maintained at a pressure of 20 mTorr and the base pressure was 2×10^{-6} Torr. A bias voltage of ~ 50 V was applied to the substrate holder during coating. The hydrocarbon and fluorinated-hydrocarbon coatings were carried out on smooth Si (1 0 0) surfaces as well as on chemically etched 6 0 6 1 Al alloy surface. The micro-nanoroughness on the Al surfaces were created by chemically etching the Al surfaces using dilute hydrochloric acid (HCl). A detailed procedure aluminum etching by HCl is described in our previous work [15]. The surface chemical compositional analyses were performed by X-ray photoelectron spectroscopy (XPS) (VGESCALAB 220iXL). The XPS spectra were collected by using a Mg K α (1253.6 eV) X-ray source. The morphological characterization was performed using an atomic force microscope (AFM) (Digital Nanoscope IIIa by Digital Instruments) and a LEO field emission scanning electron microscopy (FESEM). The wetting characteristics of the samples surfaces were carried out using a contact angle goniometer (Krüss GmbH, Germany).

3. Results and discussion

Fig. 1 shows the XPS survey spectra of hydrocarbon and fluorinated-hydrocarbon coatings deposited on a smooth Si (1 0 0) surfaces. The survey spectra confirm the presence of carbon on hydrocarbon coatings and carbon and fluorine on fluorinated-hydrocarbon coatings. A trace of oxygen was observed in both the hydrocarbon and fluorinated-hydrocarbon coatings. The additional peak of F1s at 698.17 eV in the survey spectra of fluorinated-hydrocarbon coatings (absent in case of hydrocarbon coating) is an excellent indication of the presence of fluorine in the coating originating from the combination of Ar and C₂F₆ gases used in the PECVD coating process.

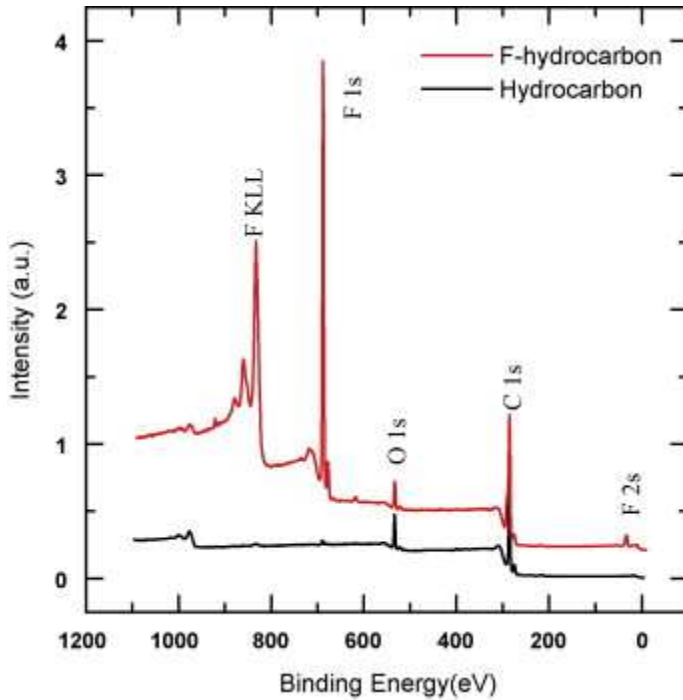


Fig. 1.

XPS surface survey spectra of hydrocarbon and fluorinated hydrocarbon coatings.

Fig. 2 shows the high-resolution C1s spectra of hydrocarbon and fluorinated-hydrocarbon coatings on smooth Si (1 0 0). It can be seen that the C1s spectra of fluorinated-hydrocarbon have been resolved into five different components, namely, –CF₃, –CF₂, –C–F, –C–CF_n and –C–C at binding energies are 292.8 eV, 290.5 eV, 288.4 eV, 287 eV and 285.0 eV, respectively as compared to only one component of –C–C at 285.0 eV in the C1s spectra of hydrocarbon coatings. The various fluorocarbon radicals in fluorinated hydrocarbon as seen in Fig. 2 obviously arise from the de-fragmentation of C₂F₆ in presence of Ar. The presence of low surface energy component such as CF₃ and CF₂ groups in the fluorinated-hydrocarbon coated surface helps lowering the surface energy.

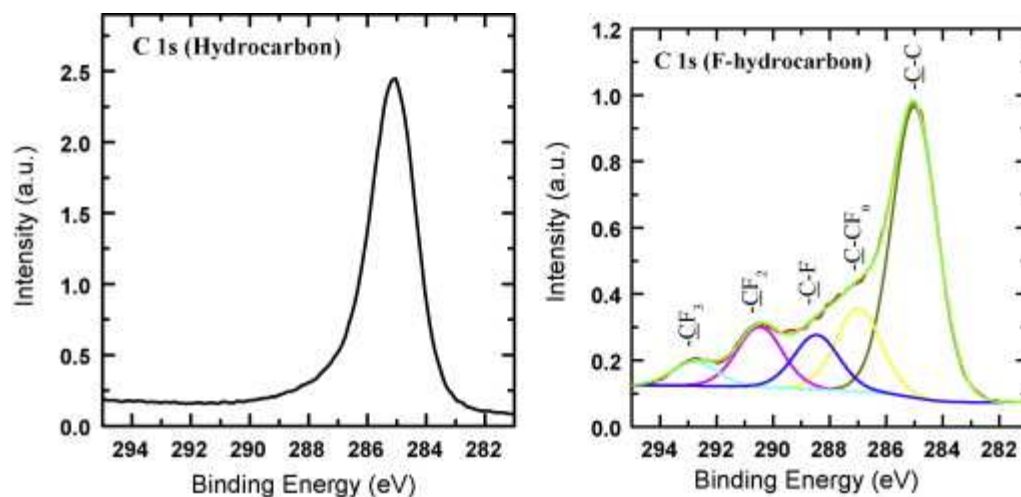


Fig. 2. XPS high-resolution C1s spectra of hydrocarbon (Ar-CH₄) and fluorinated-hydrocarbon (Ar-C₂F₆) on Si (1 0 0) surfaces.

The morphological characterization of both hydrocarbon and fluorinated-hydrocarbon coatings were performed using AFM as shown in Figs. 3a and b and 4a and b. A slight variation in the morphological features of hydrocarbon and fluorinated-hydrocarbon coating has been observed as the density of the networks in fluorinated-hydrocarbon coating (Fig. 4a and b) is comparably higher than that observed in case of hydrocarbon coating (Fig. 3a and b). A change in roughness, although minor, has also been encountered in the two coatings as the root mean square (rms) roughness of the hydrocarbon coating is ~6 nm and that of fluorinated-hydrocarbon is ~9 nm as evaluated using AFM analyses. However, the water contact angles (CA) measured on the two surfaces showed a considerable difference. The CA on the hydrocarbon coated surface was found to be ~72° (Fig. 3c) whereas the fluorinated-hydrocarbon coated surface showed a CA of ~105° (Fig. 4c). The higher CA value in case of fluorinated-hydrocarbon coated surface is due to the presence of more number of low surface energy CF₃, CF₂, etc., components as evident from XPS analyses (Fig. 2). The atomic percentage of fluorine on the surface of the fluorinated-hydrocarbon coatings was found to be ~36 at.%. The lower CA value in case of hydrocarbon coated surface is due to the absence of such low surface energy groups (CF₃, CF₂, etc.).

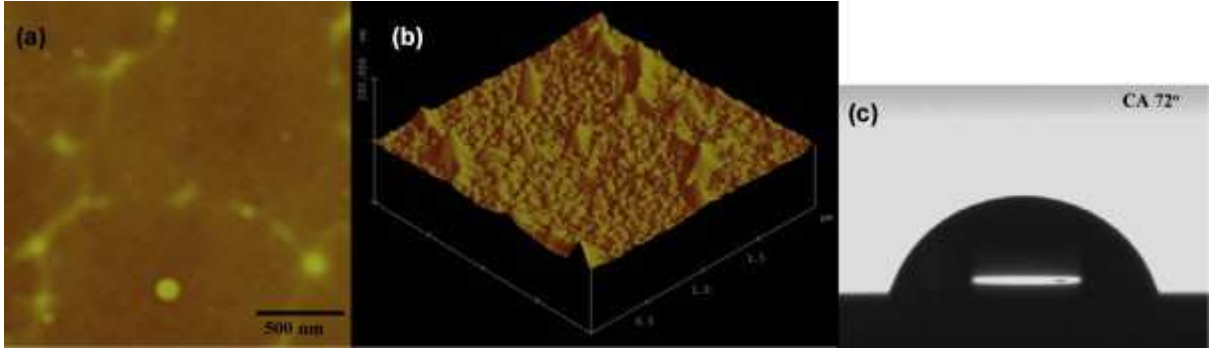


Fig. 3. (a) 2-D and (b) $2 \times 2 \mu\text{m}$ 3-D tapping mode AFM images of hydrocarbon coating on smooth Si (1 0 0) surfaces; (c) image of a water drop on hydrocarbon coated smooth Si surfaces.

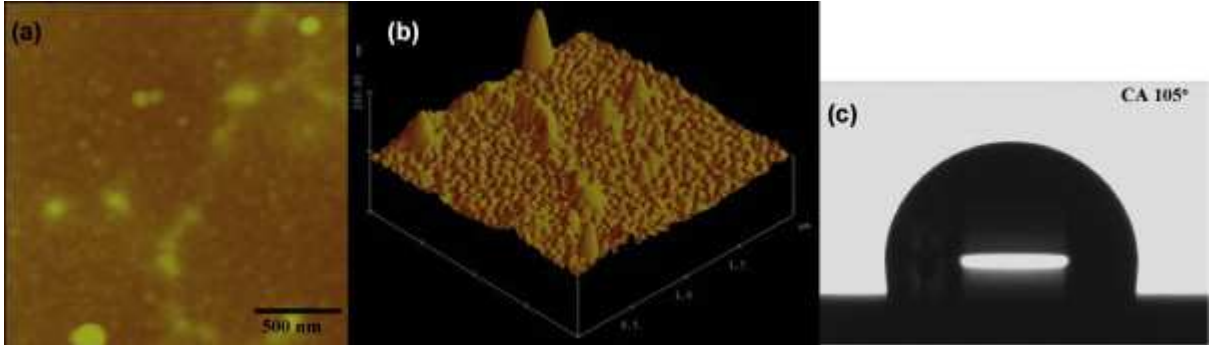


Fig. 4. (a) 2-D and (b) $2 \times 2 \mu\text{m}$ 3-D tapping mode AFM images of fluorinated-hydrocarbon coating on smooth Si (1 0 0) surfaces; (c) image of a water drop on fluorinated-hydrocarbon coated smooth Si surfaces.

Previously, Yu et al. [20] have reported the formation of fluorinated hydrocarbon using different flow ratio of CF_4/CH_4 in the PECVD process and obtained CA of 82.8° and 97.3° for hydrocarbon and fluorinated-hydrocarbon coatings, respectively. The roughness of their coatings showed an increase from 0.12 nm to 0.34 nm for a power of 100 W and 0.16 nm to 0.28 nm for the power of 60 W with varying flow rate ratio of CF_4/CH_4 from 1:4 to 4:1. They have also reported by XPS investigation that the surface composition increased with increase of CF_4 in the plasma and maximum fluorine content is found to be 30 at.% and 40 at.% for the power of 100 W and 60 W, respectively.

Another study showed that fluorinated-hydrocarbon was deposited on NiTi alloy surfaces by plasma ion implantation methods using a combination of CH₄, CF₄ and Ar plasma for studying the corrosion protection of this alloy [21]. The surface roughnesses of the coatings were found to be the function of the flux of CF₄ in the chamber and varied from 5 nm to 2.8 nm with the increase of the flux of CF₄. The maximum fluorine incorporation was reported to be 3.92 wt.% which provided a water contact angle of around 95°. A study by Uedo et al. based on similar application of corrosion resistance coatings showed that CF₄ plasma treatment has a high fluorine content (F/C:0.20) providing a surface with very low surface roughness of 0.075 nm and a water contact angle of 93°. [22].

A roughness of 0.7 nm has also been reported on the fluorinated-hydrocarbon coatings prepared using CF₄ and C₂H₂ gases with the maximum fluorine of 39 at.% [23]. However, our coatings using a mixture of Ar, and C₂F₆ gases showed a greater enhancement of water contact angle of 105° due to higher fluorine content (~36 at.%) as well as a comparably higher roughness (~9 nm) in our fluorinated-hydrocarbon coatings. To understand the behavior of the water drops on a micro-nanorough surface, the hydrocarbon and fluorinated-hydrocarbon coatings were performed on chemically etched micro-nanorough Al surfaces. The CA of the hydrocarbon coated etched aluminum surface enhanced to ~135° and the water drop stuck to those surfaces as demonstrated by the Fig. 5b making it impossible to measure the contact angle hysteresis. However, when coated with fluorinated-hydrocarbon, the micro-nanorough Al surfaces demonstrated superhydrophobic properties with CA values of ~165° and CAH of <2°. The water drops on those surfaces were found to roll-off easily even with a slightest tilt of the surfaces as observed on our previously reported rf-sputtered Teflon coated etched aluminum surfaces [15]. This observation complements the fact that the higher CA values on the fluorinated-hydrocarbon coated micro-nanorough Al surfaces as compared to that coated with hydrocarbon is due to the presence of large number of low surface energy fluorinated carbon compounds on the fluorinated-hydrocarbon coatings.

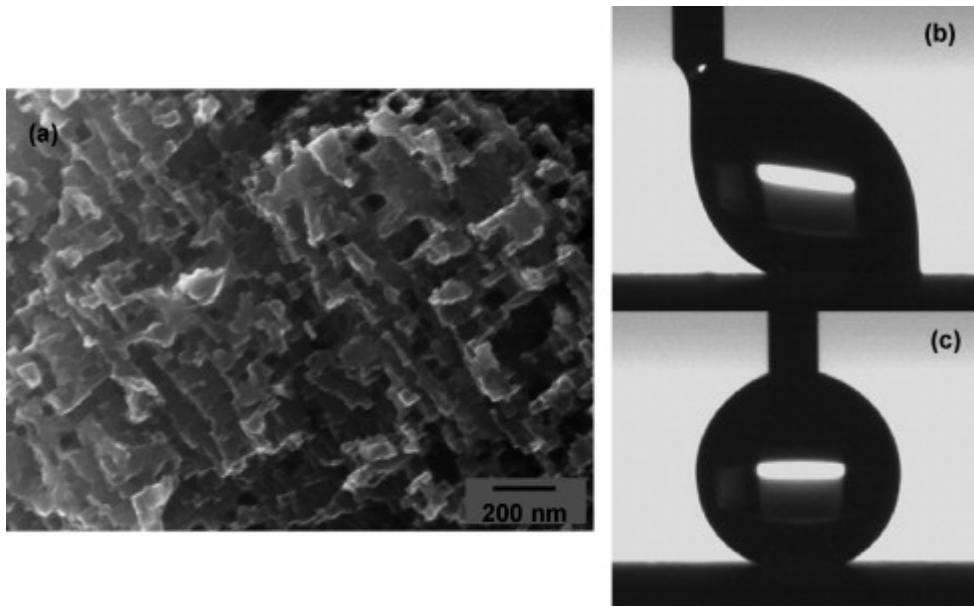


Fig. 5. (a) SEM image of micro-nanorough Al (6 0 6 1) surface; and image of a water drop suspended to a syringe needle during CAH measurements on (b) hydrocarbon coated micro-nanorough Al and (c) fluorinated-hydrocarbon coated micro-nanorough Al.

4. Conclusion

Hydrocarbon and fluorinated-hydrocarbon coatings have been deposited by plasma enhanced chemical vapor deposition technique using gaseous precursors. The morphological analyses as well as the roughness of the coatings have been carried out using AFM. Chemical compositions of the coatings were carried out using XPS. The incorporated fluorine in the fluorinated-hydrocarbon, as investigated by XPS, was found to be ~ 36 at.%. The contact angle of water on the hydrocarbon coated on silicon surface has been found to be 72° and that has been enhanced to 105° in case of fluorinated-hydrocarbon coatings. Contact angle of $\sim 135^\circ$ and $\sim 165^\circ$, respectively, have been achieved by depositing these coatings on chemically etched micro-nanorough aluminum surfaces. The fluorinated-hydrocarbon coated etched aluminum substrate has shown a contact angle hysteresis of below 2° with the rolling off water drop as compared to the hydrocarbon coated rough surface on which the water drop stuck. The difference in their wetting behavior is attributed to the presence of high fluorine content in case of fluorinated-hydrocarbon coatings and the absence of such fluorine content in case of the hydrocarbon coatings.

Acknowledgements

This work was carried out within the framework of the NSERC/Hydro-Quebec/UQAC Industrial Chair on Atmospheric Icing of Power Network Equipment (CIGELE) and the Canada Research Chair on Engineering of Power Network Atmospheric Icing (INGIVRE) at Université du Québec à Chicoutimi. The authors would like to thank the Institut national de recherche scientifique (INRS), as well as CIGELE partners (Hydro-Québec, Hydro One, Réseau Transport d'Électricité (RTE) and Électricité de France (EDF), Alcan Cable, K-Line Insulators, Tyco Electronics, Dual-ADE, CQRDA and FUQAC) whose financial support made this research possible.

References

- [1] A. Scardino, R. De Nys, O. Ison, W. O'Connor, P. Steinberg
Biofouling, 19 (2003), p. 221
- [2] J.D.J.S. Samuel, P. Ruther, H.-P. Frerichs, M. Lehmann, O. Paul, J. Ruhe
Sens. Actuators B, 110 (2005), p. 218
- [3] A. Singh, L. Steely, H.R. Allcock
Polym. Prepr. (ACS Div. Polym. Chem.), 46 (2005), p. 599
- [4] H. Gau, S. Herminghaus, P. Lenz, R. Lipowsky
Science, 283 (1999), p. 46
- [5] T. Liu, Y. Yin, S. Chen, X. Chang, S. Cheng
Electrochim. Acta, 52 (2007), p. 3709
- [6] D. Quéré
Rep. Prog. Phys., 68 (2005), p. 2495
- [7] K. Satoh, H. Nakazumi
J. Sol-Gel Sci. Technol., 27 (2003), p. 327
- [8] T. Kako, A. Nakajima, H. Irie, Z. Kato, K. Uematsu, T. Watanabe, K. Hashimoto
J. Mater. Sci., 39 (2004), p. 547
- [9] A. Nakajima, K. Hashimoto, T. Watanabe
Monatshefte für Chemie, 132 (2001), p. 31
- [10] W. Barthlott, C. Neinhuis
Planta, 202 (1997), p. 1
- [11] A.B.D. Cassie, S. Baxter
Trans. Faraday Soc., 40 (1944), p. 546

- [12] M. Ma, M.R. Hill
Curr. Opin. Colloid Interf. Sci., 11 (2006), p. 193
- [13] A. Safaee, D.K. Sarkar, M. Farzaneh
Appl. Surf. Sci., 254 (2008), p. 2493
- [14] D.K. Sarkar, M. Farzaneh
J. Adhesion Sci. Technol., 23 (2009), p. 1215
- [15] D.K. Sarkar, M. Farzaneh, R.W. Paynter
Mater. Lett., 62 (2008), p. 1226
- [16] D.K. Sarkar, M. Farzaneh
Appl. Surf. Sci., 254 (2008), p. 3758
- [17] D.K. Sarkar, M. Farzaneh
K.L. Mittal (Ed.), Contact Angle, Wettability and Adhesion,, vol.5VSP/Brill, Leiden (2008),
pp. 271–278
- [18] N. Saleema, D.K. Sarkar, M. Farzaneh
K.L. Mittal (Ed.), Contact Angle, Wettability and Adhesion,, vol.5VSP/Brill, Leiden (2008),
pp. 279–285
- [19] N. Saleema, M. Farzaneh
Appl. Surf. Sci., 254 (2008), p. 2690
- [20] G.Q. Yu, B.K. Tay, Z. Sun
Surf. Coat. Technol., 191 (2005), p. 236
- [21] J.H. Sui, Z.G. Zhang, W. Cai
Nucl. Inst. Method. B, 267 (2009), p. 2475
- [22] A. Ueda, D. Kato, N. Sekioka, T. Kamata, R. Kurita, H. Uetsuka, Y. Hattori, S.
Hirono, S. Umemura, O. Niwa
Carbon, 47 (2009), p. 1943
- [23] C.-H. Lai, W.-S. Lai, H.-C. Chiue, H.-J. Chen, S.-Y. Chang, S.-J. Lin
Thin Solid Films, 510 (2006), p. 125